Controlling the carrier-envelope phase of few-cycle focused laser beams with a dispersive beam expander

Carlos J. Zapata-Rodríguez and Miguel A. Porras

Departamento de Óptica, Universidad de Valencia, 46100 Burjassot, Spain.
Departamento de Física Aplicada, ETSIM, Universidad Politécnica de Madrid, Ríos Rosas 21, 28003 Madrid, Spain.

Abstract: We report on a procedure to focalize few-cycle laser pulses in dispersive media with controlled waveform. Stationarity of the carrier-envelope phase for extended depth of focus is attained by shaping the spatial dispersion of the ultrashort beam. An adjustable group velocity is locally tuned in order to match a prescribed phase velocity at focus. A hybrid diffractive-refractive lens system is proposed to drive the wavefield to an immersion microscope objective under convenient broadband modulation. Numerical simulations demonstrate robustness over positioning of this dispersive beam expander.

References and links

1. A. Rubinowicz, "On the anomalous propagation of phase in the focus," J. Opt. Soc. Am. **54**, 931–936 (1938).
2. R. W. Boyd, "Intuitive explanation of the phase anomaly of focused light beams," J. Opt. Soc. Am. **70**, 877–880 (1980).
3. S. Feng and H. G. Winful, "Physical origin of the Gouy phase shift," Opt. Lett. **26**, 485–487 (2001).
4. L. G. Gouy, "Sur une propriété nouvelle des ondes lumineuses," Compt. Rendue Acad. Sci. (Paris) **110**, 1251–1253 (1890).
5. M. A. Porras, "Diffraction effects in few-cycle optical pulses," Phys. Rev. E **65**, 026,606 (2002).
6. S. Feng, H. G. Winful, and R. W. Hellwarth, "Gouy shift and temporal reshaping of focused single-cycle electromagnetic pulses," Opt. Lett. **23**, 385–387 (1998).
7. Z. L. Horváth and Z. Bor, "Reshaping of femtosecond pulses by the Gouy phase shift," Phys. Rev. E **60**, 2337–2346 (1999).
8. A. B. Ruffin, J. V. Rudd, J. F. Whitaker, S. Feng, and H. G. Winful, "Direct observation of the Gouy phase shift with single-cycle Terahertz pulses," Phys. Rev. Lett. **83**, 3410–3413 (1999).
9. F. Lindner, G. G. Paulus, H. Walther, A. Baltuška, E. Goulielmakis, M. Lezius, and F. Krausz, "Gouy phase shift for few-cycle laser pulses," Phys. Rev. Lett. **92**, 113,001 (2004).
10. T. Tritschler, K. D. Hof, M. W. Klein, and M. Wegener, "Variation of the carrier-envelope phase of few-cycle laser pulses owing to the Gouy phase: a solid-state-based measurement," Opt. Lett. **30**, 753–755 (2005).
11. E. Goulielmakis, M. Uiberacker, R. Kienberger, A. Baltuska, V. Yakovlev, A. Scrinzi, T. Westerwalbesloh, U. Kleineberg, U. Heinzmann, M. Drescher, and F. Krausz, "Direct measurement of light waves," Science **305**, 1267–1269 (2004).
12. S. E. Irvine, P. Dombi, G. Farkas, and A. Elezzabi, "Influence of the carrier-envelope phase of few-cycle pulses on ponderomotive surface-plasmon electron acceleration," Phys. Rev. Lett. **97**, 146,801 (2006).
13. P. Dombi and P. Rácz, "Ultrafast monoenergetic electron source by optical waveform control of surface plasmons," Opt. Express **16**, 2887–2893 (2008).
14. M. A. Porras, C. J. Zapata-Rodríguez, and I. Gonzalo, "Gouy wave modes: undistorted pulse focalization in a dispersive medium," Opt. Lett. **32**, 3287–3289 (2007).

15. C. J. Zapata-Rodríguez and M. T. Caballero, "Ultrafast beam shaping with high-numerical-aperture microscope objectives," Opt. Express **15**, 15,308–15,313 (2007).
16. C. J. Zapata-Rodríguez and M. T. Caballero, "Isotropic compensation of diffraction-driven angular dispersion," Opt. Lett. **32**, 2472–2474 (2007).
17. C. J. Zapata-Rodríguez, M. T. Caballero, and J. J. Miret, "Angular spectrum of diffracted wave fields with apochromatic correction," Opt. Lett. **33**, 1753–1755 (2008).
18. T. E. Sharp and P. J. Wisoff, "Analysis of lens and zone plate combinations for achromatic focusing of ultrashort laser pulses," Appl. Opt. **31**, 2765–2769 (1992).
19. E. Ibragimov, "Focusing of ultrashort laser pulses by the combination of diffractive and refractive elements," Appl. Opt. **34**, 7280–7285 (1995).
20. G. M. Morris, "Diffraction theory for an achromatic Fourier transformation," Appl. Opt. **20**, 2017–2025 (1981).
21. G. Mínguez-Vega, E. Tajahuerce, M. Fernández-Alonso, V. Climent, J. Lancis, J. Caraquitena, and P. Andrés, "Dispersion-compensated beam-splitting of femtosecond light pulses: Wave optics analysis," Opt. Express **15**, 278–288 (2007).
22. M. A. Porras, G. Valiulis, and P. D. Trapani, "Unified description of Bessel X waves with cone dispersion and tilted pulses," Phys. Rev. E **68**, 016,613 (2003).
23. C. J. Zapata-Rodríguez, "Debye representation of dispersive focused waves," J. Opt. Soc. Am. A **24**, 675–686 (2007).
24. A. E. Siegman, *Lasers* (University Science Books, Mill Valley, 1986).
25. C. J. Zapata-Rodríguez, "Focal waveforms with tunable carrier frequency using dispersive aperturing," Opt. Commun. **281**, 4840–4843 (2008).
26. V. Moreno, J. F. Román, and J. R. Salgueiro, "High efficiency diffractive lenses: Deduction of kinoform profile," Am. J. Phys. **65**, 556–562 (1997).
27. J. M. Bendickson, E. N. Glytsis, and T. K. Gaylord, "Metallic surface-relief on-axis and off-axis focusing diffractive cylindrical mirrors," J. Opt. Soc. Am. A **16**, 113–130 (1999).
28. C. Oh and M. J. Escuti, "Achromatic diffraction from polarization gratings with high efficiency," Opt. Lett. **33**, 2287–2289 (2008).

1. Introduction

The so-called Gouy phase is the subject of continuous investigation since in 1890 Louis G. Gouy published a celebrated paper on the longitudinal phase delay of spherical beams. Its relevance is primarily purely academic; for instance, the superluminal phase velocity found in the focal region of paraxial Gaussian beams may be understood in terms of this phase anomaly. Direct observation of Gouy phases has attracted the interest more recently in the framework of single-cycle focused beams . In this context, on the contrary, it results of great importance for a wide variety of phenomena and applications involving high field physics and extreme nonlinear optics. The key point to highlight here is that Gouy phase dispersion is determinant in the waveform of broadband optical pulses [5], which is commonly parametrized by the carrier-envelope phase (CEP). Sensitivity to CEP is observed for instance in photoionization of atoms and in photoelectron acceleration at metal surfaces mediated by surface plasmon polaritons

In general, focused pulses manifest strong phase dispersion along the focal region, so that enhanced spatial resolution is achieved in CEP-dependent phenomena. In some circumstances, however, increased depth of focus may be of convenience so that a stationary CEP should be required near the focus. It is remarkable that Gouy waves modes show some control over on-axis phases demonstrating undistorted pulse focalization even in dispersive media. Practical realizations are driven by angular dispersion engineering of ultrashort laser beams. In this concern we have recently introduced the concept of dispersive imaging as a tool for controlling the dispersive nature of broadband wavefields. Achromatic and apochromatic corrections of the angular spectrum of diffracted wavefields may be achieved with the use of highly-dispersive lenses such as kinoform-type zone plates. Incidentally, this is not a new idea; compensation of longitudinal chromatic aberrations [18, 19] and also diffraction-induced chromatic mismatching of Fraunhofer patterns have been proposed elsewhere.

In this paper we exploit dispersive imaging assisted by zone plates to gain control over the

waveforms of focused laser beams as approaches to Gouy waves modes. For simplicity, the theoretical analysis is addressed to pulse Gaussian beams. We perform a lens system design using the $ABCD$ matrix formalism providing fundamental attributes of a dispersive beam expander capable of adjusting conveniently the spatial dispersion of the collimated input beam. Finally, numerical simulations show CEP stationarity of few-cycle focused pulses in dispersive media along the optical axis near the focus.

2. Background

Let us consider a focused pulse. If we neglect pulse envelope distortion in the focal volume, a reasonable statement based on the short-path propagation in the region of interest, the on-axis temporal evolution of the (real) field can be conveniently given as

$$E(t,z) = E_0(t')\cos(\omega_0 t' - \phi_0), \tag{1}$$

where $t' = t - \dot{\varphi}_0$ denotes a local time, $\phi_0 = \varphi_0 - \omega_0\dot{\varphi}_0$ is the carrier-envelope phase being $\varphi(z,\omega)$ the complex argument of the spectrum and ω_0 the carrier frequency. In the following, a dot over a parameter stands for a derivative with respect to ω, and a subscript 0 denotes its evaluation at the specific frequency $\omega = \omega_0$; therefore, the carrier phase φ_0 symbolizes $\varphi(z,\omega_0)$ and the envelope delay $\dot{\varphi}_0$ represents $\partial_\omega\varphi$ computed at $\omega = \omega_0$. Rigorously speaking, Eq. (1) is a sufficiently general expression and its validity is restricted to pulse envelopes E_0 described by symmetric even functions.

Stationarity of the CEP, i.e. conservation of ϕ_0 along with the z coordinate, entails a spatiotemporal evolution of the field E expressed in terms of an spatially-invariant waveform (irrespective of its amplitude). In free space, a rigorous stationary CEP has been reported solely for X-waves However, finite-energy focal pulses demonstrate a variation of ϕ_0 upon z due to material dispersion and, importantly, the presence of the Gouy phase. At most, a stationary CEP may be achieved in a small region around a point of interest (the focal point) reaching the stationarity condition $\partial_z\phi_0 = 0$. We conveniently introduce the local wavenumber $k_z(z,\omega) = \partial_z\varphi$; we point out that on-axis pulse propagation evolves at a local phase velocity $v_p(z) = \omega_0/k_{z0}$ and group velocity $v_g(z) = \dot{k}_{z0}^{-1}$. Therefore

$$\partial_z\phi_0 = \omega_0\left(\frac{1}{v_p} - \frac{1}{v_g}\right), \tag{2}$$

and CEP stationarity is attained when the phase velocity matches the group velocity, $v_p = v_g$, (both denoted as v). In this case, and assuming the focal point is located at $z = 0$, the spatial-temporal dynamics of E in its vicinity may be given in terms of the variable $t - z/v$. Indeed, this result is more general as derived here.

3. Stationarity of CEP in focus

For illustration, we consider a focused Gaussian beam of waist (and focus) at $z = 0$ propagating through a nonabsorbing dielectric medium of refractive index $n_p = ck/\omega$. The on-axis wavefield of time-harmonic dependence $\exp(-i\omega t)$ results

$$\varepsilon(\omega,z) = \frac{z_R\exp(ikz)}{iq}\varepsilon(\omega,0), \tag{3}$$

where $q(\omega,z) = z - iz_R$ is the complex radius of curvature, $z_R = ks^2/2$ is the Rayleigh range (s is the size of the beam waist), and $\varepsilon(\omega,0)$ is the focal spectrum. The argument of the complex

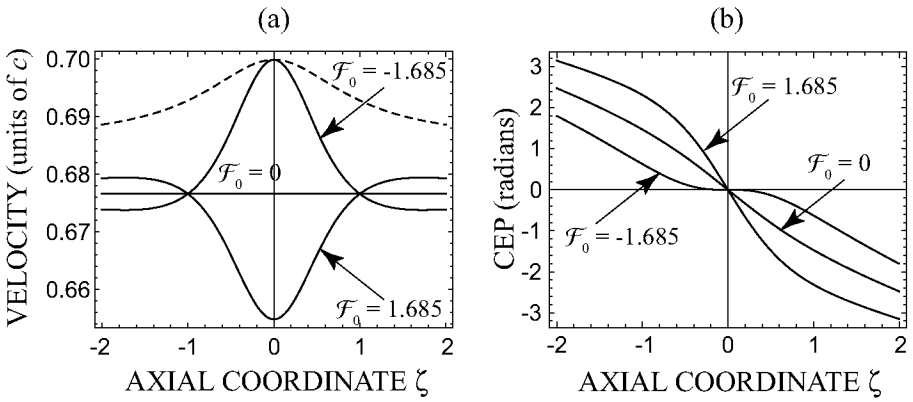

Fig. 1. Phase velocity (dashed line) and group velocity (solid lines) represented in (a) for pulsed Gaussian beams of different $\mathcal{F}_0$ ($\mathcal{L}_0 = 34$) propagating in fused silica at $\omega_0 = 3.14\ \mathrm{fs}^{-1}$. In (b) we also show the CEP evolution along the optical axis.

field ε (omitting irrelevant terms) is $\varphi = kz - \varphi_G$, being $\varphi_G = \arctan(z/z_R)$ the Gouy phase. Finally, the Gaussian local wavenumber is

$$k_z = k - \frac{z_R}{z^2 + z_R^2}, \tag{4}$$

which is lower than the wavenumber k associated with a plane wave.

Particularly, the phase velocity of the Gaussian beam in terms of the normalized axial coordinate $\zeta = z/z_{R0}$ is

$$v_p = c\left[n_{p0} - \frac{1}{\mathcal{L}_0(1+\zeta^2)}\right]^{-1}, \tag{5}$$

where z_{R0} is the Rayleigh range at ω_0 and the Gaussian length $\mathcal{L} = kz_R/n_p$. Note that $\mathcal{L}_0 = k_0^2 s_0^2/2n_{p0}$ also gives the area (conveniently normalized) of the beam waist at ω_0. On the other hand, the group velocity yields

$$v_g = c\left[n_{g0} + \frac{\mathcal{F}_0(1-\zeta^2)}{\mathcal{L}_0(1+\zeta^2)^2}\right]^{-1}, \tag{6}$$

where $n_g = c\dot{k}$ is the group index, and $\mathcal{F} = \omega \dot{z}_R/z_R$. In order to understand its significance, let us conceive a Gaussian beam exhibiting an invariant $\mathcal{F}$ within a given spectral band around ω_0; this case would consider a dispersive Rayleigh range $z_R = z_{R0}(\omega/\omega_0)^{\mathcal{F}}$, a model employed elsewhere [10]. Therefore, $\mathcal{F}$ parametrizes the longitudinal dispersion of the Gaussian beam; this can be deduced also from the relationship $\mathcal{F} = \omega \dot{\mathcal{L}}/\mathcal{L} - 1$. More importantly, velocity matching $v_p = v_g$ at focus is found if

$$\mathcal{F}_0 = -(1 + \mathcal{L}_0 \Delta n_0), \tag{7}$$

being $\Delta n = n_g - n_p$ the difference of group index and refractive index in the dispersive medium. Equivalently Eq. (7) reads $\dot{\mathcal{L}}_0 = -\mathcal{L}_0^2 \Delta n_0/\omega_0$. We conclude that CEP stationarity requires a given spatial dispersion of the wavefield to balance dispersion of the dielectric material Δn_0. In particular, $\Delta n = 0$ in vacuum and therefore $\mathcal{F} = -1$, independently of the beam length.

In Fig. 1(a) we compare graphically the phase velocity and the group velocity of pulse Gaussian beams of $\mathcal{L}_0 = 34$ with several ratios $\mathcal{F}_0$ propagating in fused silica. At the mean

frequency $\omega_0 = 3.14\ \mathrm{fs}^{-1}$ we have $n_{p0} = 1.458$ and $n_{g0} = 1.478$. As expected, isodiffracting Gaussian beams evidencing an invariant Rayleigh range ($\mathscr{F} = 0$) exhibit a constant group velocity along the optical axis. Of particular importance is the case $\mathscr{F}_0 = -1.685$ obtained from Eq. (7), since phase and group velocities matches at the focal point. In this case the CEP, written with zero initial phase ($\phi_0 = 0$ at $\zeta = 0$) as

$$\phi_0(\zeta) = -\arctan(\zeta) - \mathscr{L}_0 \Delta n_0 \zeta - \mathscr{F}_0 \frac{\zeta}{\zeta^2 + 1}, \tag{8}$$

proves stationarity features at the origin, where $\partial_\zeta \phi_0 = 0$, as shown in Fig. 1(b). Moreover, Eq. (7) leads the on-axis CEP evolution to ultraflattened curves in the focal region since, in fact, $\zeta = 0$ is a saddle point where $\partial_\zeta^2 \phi_0 = 0$. Consequently, a quasi-matching of phase and group velocities is also demonstrated in the neighborhood of the focus. At the boundaries of the focal volume, $|\zeta| = 1$, a significant mismatch of velocities is clear, which is quantitatively equivalent for different values of $\mathscr{F}_0$. However, the CEP accumulates monotonically (in our numerical examples) such differences, in a certain way, displaying the mismatch history of the phase and group velocities and, as a consequence, the CEP provides its lowest (absolute) value for $\mathscr{F}_0 = -1.685$ in Fig. 1(b).

4. Optical system

Established that focalization of ultrashort laser beams is commonly produced with a CEP running loosely within the focal depth, here we analyze a procedure inducing controlled spatial dispersion to achieve a stationary CEP. We assume the (collimated) laser Gaussian beam, of input Rayleigh range $z_{Rin} = \omega s_{in}^2/2c$, propagates in vacuum and impinges over an objective lens in order to produce the required focused field of z_R embedded in a medium of refractive index n_p. For convenience we assume a nondispersive infinity-corrected microscope objective of focal length f, and also beam truncation is ignored. Under the Debye approximation, the width of the Gaussian beam at the back focal plane

$$s = \frac{2f}{k s_{in}}, \tag{9}$$

provided the Rayleigh range of the focused beam $z_R \ll f$. In this model, the focused laser beam is free of low-Fresnel-number focal shifts and longitudinal chromatic aberrations. As a consequence, the Gaussian lengths of the input ($\mathscr{L}_{in}$) and focused ($\mathscr{L}$) beams satisfies $\mathscr{L}_{in}\mathscr{L} = \omega^2 f^2/c^2 n_p$, whereas longitudinal dispersion of the fields obeys $\mathscr{F}_{in} + \mathscr{F} = -\Delta n/n_p$. Rather than concerning the focused pulse, we cast Eq. (7) showing explicitly the CEP constraint for the input Gaussian beam instead, yielding

$$\mathscr{F}_{in0} = 1 + \frac{\Delta n_0}{n_{p0}} \left(\frac{\omega_0^2 f^2}{c^2 \mathscr{L}_{in0}} - 1 \right). \tag{10}$$

As a consequence, dispersive tailoring of the laser beam reaching $\mathscr{F}_{in0}$ of Eq. (10) leads to CEP stationarity near the focus of the converging field. If focusing is performed in vacuum ($\Delta n_0 = 0$), $\mathscr{F}_{in} = 1$ characterizing input pulsed fields of a Gaussian width that is independent upon the frequency, on other hand a well-established assumption in numerous studies.

When focusing is carried out in dispersive bulk media, apparently, Eq. (10) is not generally satisfied for the input laser beam. In principle, modification of f and $\mathscr{L}_{in0}$ with different microscope objectives and beam expanders may result of practical convenience; however, these laser-beam tunes are produced at the cost of a field resizing at focus. This is evident if we

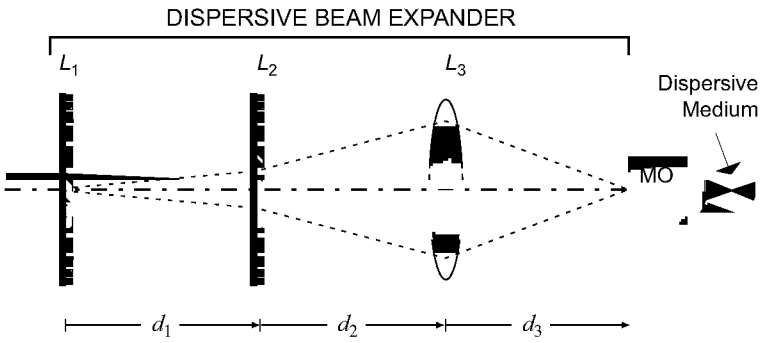

Fig. 2. Schematic diagram of the focusing setup: L_1 and L_2 are components of the diffractive doublet; L_3 is the refractive lens and MO is the microscope objective.

express Eq. (10) as $\mathscr{F}_{in0} = 1 + \Delta n_0 \left(\mathscr{L}_0 - n_{p0}^{-1} \right)$. In a majority of applications this is undesirable. We might conserve typical lengths of inputs and focused beams at ω_0 if, alternatively, spatial dispersion of the laser pulse is altered modifying $\mathscr{F}_{in0}$. In this case we switch the group velocity of the pulse at focus in order to match the given phase velocity. Next we propose an optical arrangement specifically designed to convert a given (collimated) pulsed Gaussian beam of Gaussian length $\tilde{\mathscr{L}}_{in0}$ and dispersion $\tilde{\mathscr{F}}_{in0}$, violating Eq. (10), into an ultrashort collimated laser beam of the same length $\mathscr{L}_{in0} = \tilde{\mathscr{L}}_{in0}$ but $\mathscr{F}_{in0}$ satisfying Eq. (10), as a previous step to the focusing action performed by the microscope objective.

First we may give general features of the required system using the $ABCD$ matrix formalism. A perfect replica (image) of the Gaussian beam is generated if we impose $B = 0$ and $C = 0$, simultaneously. This afocal system provides a lateral magnification $A = D^{-1}$ of the image and, therefore, $z_{Rin} = A^2 \tilde{z}_{Rin}$ is inferred. From $\tilde{\mathscr{L}}_{in0} = \mathscr{L}_{in0}$ we derive that $A_0^2 = 1$; that is, beam expansion is unitary at ω_0. Also we obtain that

$$\mathscr{F}_{in0} = \tilde{\mathscr{F}}_{in0} + \frac{2\omega_0 \dot{A}_0}{A_0}. \tag{11}$$

As a consequence, dispersion of the matrix element A is required in order to change the spatial dispersion properties of the Gaussian beam, switching from $\tilde{\mathscr{F}}_{in0}$ to $\mathscr{F}_{in0}$. This is of relevance also concerning the temporal response of the $ABCD$ system; the spectrum of the field at the output plane is altered being multiplied by the spectral modifier A^{-1}. Under strong corrections at this preprocessing stage, the spectrum of the collimated laser beam may be greatly distorted

Ultimately, a spectral shift of the mean (carrier) frequency may be induced, which urges to recalculate Eq. (10); this effect is neglected here.

We propose the spatio-spectral processing of the Gaussian beam to be performed by the thin-lens triplet depicted in Fig. 2. This is inspired in the setup shown . Firstly we introduce a doublet composed of kinoform-type zone plates (L_1 and L_2 in the plot) of dispersive focal lengths $f_1 = f_{10}\omega/\omega_0$ and $f_2 = f_{20}\omega/\omega_0$, respectively, followed by a nondispersive refractive lens (L_3) of focal length $f_3 = f_{30}$. Phase-only diffractive lenses may have nearly-100% efficiency at ω_0; neglecting losses due for instance to material absorption and reflections, the kinoform-lens efficiency may be estimated as [26]

$$\eta(\omega) = \mathrm{sinc}^2 \left(\frac{\omega}{\omega_0} - 1 \right), \tag{12}$$

where $\mathrm{sinc}(x) = \sin(\pi x)/(\pi x)$. We point out that Eq. (12) ignores material chromatic dispersion in the lens to simplify our discussion; this assumption may be given in practice using for

instance a diffractive mirror Therefore, the strength of the response η decreases severely at increasing spectral shifts due to the appearance of undesirable diffraction orders. This is a relevant effect for subcycle pulses, however being negligible in ultrashort beams of sufficiently narrow power spectrum as considered below. Interestingly, diffractive optical elements with high-efficiency responses, significantly flatter than η from Eq. (12) and spanning the visible wavelength range, have been reported using twisted nematic liquid crystals.

We point out that the matrix elements are necessarily dispersive in virtue of the ω-dependent character of f_1 and f_2. The coupling distance of the diffractive doublet is d_1, and the distance from L_2 to L_3 is d_2. Furthermore, we assume that L_1 is placed at the waist plane of the input Gaussian beam of Rayleigh range $\tilde{z}_{Rin}$. After propagating through the triplet, the output field of dispersion-compensated $z_{Rin} = -\mathrm{Im}\{q_{in}\}$ is examined at a distance

$$d_3 = \frac{[d_1 d_2 - (d_1 + d_2) f_2] f_3}{d_1(d_2 - f_2 - f_3) + f_2(f_3 - d_2)} \tag{13}$$

from L_3 where the waist image is found ($B = 0$). For completeness, let us remind the well-known matrix equation for Gaussian beams

$$q_{in} = \frac{A\tilde{q}_{in} + B}{C\tilde{q}_{in} + D}, \tag{14}$$

being $\tilde{q}_{in} = -i\tilde{z}_{Rin}$ the complex radius of the input laser beam at the plane of L_1.

Distance d_3 depends upon ω so that we have control over the waist location of the imaged Gaussian beam for a single frequency. This is of concern when placing the microscope objective; thus let us impose d_3 at $\omega = \omega_0$ to be the distance from L_3 to the objective lens (see Fig. 2). This longitudinal chromatic dispersion of the waist plane leads to a dispersive spherical wavefront in the entrance plane of the objective. Ultimately this fact yields a longitudinal chromatic aberration of the broadband focused wavefield that may be neglected upon evaluation of the Gaussian Fresnel number $N_G = \mathrm{Re}\{q_{in}\}/z_{Rin}$ of the beam impinging onto the objective lens; specifically $|N_G| \ll 1$ should be satisfied.

Collaterally, a parametric solution satisfying, simultaneously, $B = 0$ and $C = 0$ cannot be found. A sufficient condition may be established by imposing $C_0 = 0$ and $\dot{C}_0 = 0$ so that C vanishes in the vicinity of the carrier frequency. Such a tradeoff is given when

$$f_3 = d_2 + \frac{(d_1 - f_{10})^2}{d_1}, \tag{15}$$

$$f_{20} = -\frac{(d_1 - f_{10})^2}{f_{10}}. \tag{16}$$

This approach suggests that afocality of the the imaging setup is not rigorous but stationary around $\omega = \omega_0$.

Finally $d_2 = f_{10} - d_1$ yields an unitary magnification $A_0 = 1$; alternatively we may consider $d_2 = 3f_{10} - d_1 - 2f_{10}^2/d_1$ giving $A_0 = -1$. Additionally, if

$$f_{10} = d_1 \left(1 + \frac{2}{\Delta\mathscr{F}_{in0}}\right) \tag{17}$$

(in both cases), where the mismatching $\Delta\mathscr{F}_{in0} = \mathscr{F}_{in0} - \tilde{\mathscr{F}}_{in0}$, then $\dot{A}_0 = A_0 \Delta\mathscr{F}_{in0}/2\omega_0$ as requested in (11). We conclude that the focal length of each lens composing the hybrid diffractive-refractive triplet is determined by the parameter $\Delta\mathscr{F}_{in0}$ and the positive axial distance d_1. This particular procedure cannot be applied if $-4 \leq \Delta\mathscr{F}_{in0} < 0$ demanding a negative value of the

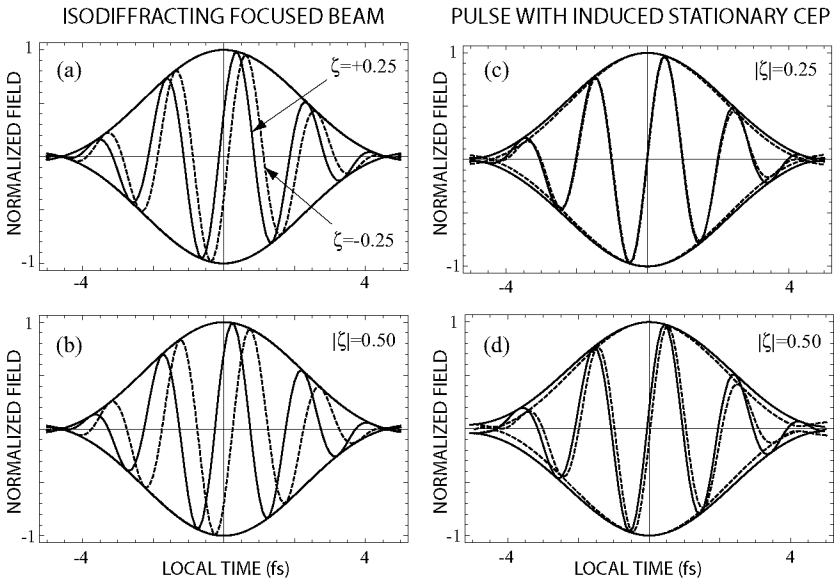

Fig. 3. Evolution of the wavefield and envelope at different on-axis points ζ of the focal volume. Negative values of ζ are drawn in dashed lines and positive values in solid lines. Subfigures (a)–(b) correspond to isodiffracting Gaussian beams focused onto bulk fused silica. Time domain is given in terms of the local time t'. In (c)–(d) we employ a CEP-stationarity procedure.

axial distance d_2. In these cases we might consider a different arrangement: a triplet with L_1 being a nondispersive thin lens and L_3 a zone plate instead. Following the analysis given above, it can be proved that a satisfactory dispersive processing is also provided using positive values of d_1 and d_2 in the interval $\Delta\mathscr{F}_{in0} < 0$.

5. Numerical verification

Let us illustrate the validity of our approach with a numerical simulation. We consider an isodiffracting Gaussian beam focused by a microscope objective lens of $f = 4$ mm, which propagates in fused silica near the focus. From a practical point of view, oil-immersion objectives are suitable to get rid of longitudinal chromatic aberration and focal shifts. Input widths $s_{in} = 0.8$ mm ($\mathscr{L}_{in0} = 3.5\ 10^7$) allow that aperturing may be neglected in immersion objectives of NA > 0.75. Numerical computations are performed with the Fresnel-Kirchhoff diffraction formula. At focus we employ a bandlimited signal ε of normalized (amplitude) spectrum $1 - 2\Omega^2 + \Omega^4$ for $|\Omega| < 1$, where $\Omega = (\omega - \omega_0)/\Delta_0$. The mean frequency is $\omega_0 = 3.14$ fs^{-1} and the width of the spectral window is $0.8\omega_0$, i.e. $\Delta_0 = 0.4\omega_0$, providing a 4.8 fs (FWHM) transform-limited optical pulse. Figures 3(a) and 3(b) show on-axis waveforms near the focal point. The field envelopes are unaltered in spite of material dispersion; however, the carrier shifts inside the envelope in response of the velocity mismatching, $v_p = 0.700c$ and $v_g = 0.677c$, evaluated at focus.

Insertion of the dispersive beam expander of Fig. 2 provides focal waveforms shown in Figs. 3(c) and 3(d). The contribution due to unwanted higher orders of a given kinoform lens is neglected; considering an input signal s like that observed at focus, ε, the integrated (mean)

efficiency for the output,

$$\overline{\eta} = \frac{\int_{-1}^{1} |s|^2 \eta \, d\Omega}{\int_{-1}^{1} |s|^2 d\Omega}, \tag{18}$$

theoretically reaches a value $\overline{\eta} = 0.954$, revealing that higher-order foci carry only 4.6% of the input intensity. Correspondingly, the spectral amplitude shaping on the transmitted beam may be disregarded; the spectral modifier $\sqrt{\eta}$ altering the input signal s through a kinoform zone plate would induce a small pulse stretching (from 4.8 fs) up to 4.9 fs FWHM. We observe that CEP is significantly stabilized around the focus, where $\mathscr{L}_0 = 34$ and $\mathscr{F}_0 = -1.685$. In order to minimize the Fresnel number, we have selected $d_1 = 200$ mm (for $A_0 = 1$) giving $|N_G| < 0.4$ in our spectral window. Eqs. (15)–(17) yield values for the focal distances of the triplet, $f_{10} = 439$ mm, $f_{20} = -130$ mm, and $f_3 = 525$ mm; also $d_2 = f_{10} - d_1 = 239$ mm. Importantly, evaluation of Eq. (13) provides a negative axial distance at ω_0; this incongruency is overcome placing the microscope objective immediately behind L_3 ($d_3 = 0$), as considered in the numerical simulations. This procedure is robust since such an adjustment still maintains the value of v_g switched up to $0.700c$; however, a minor asymmetric pulse broadening is observable. We point out that a relay system might be employed in cases where pulse distortions are dramatic. Placed between the dispersive beam expander and the microscope objective, the relay system may translate the appropriately-corrected virtual pattern of the broadband Gaussian pulse to the entrance plane of the focusing element.

6. Conclusions

In summary, we investigate the problem of focusing a few-cycle optical field with stationarity of the signal within the depth of focus. Following theoretical concerns, we establish basic requirements for an optical setup to drive pulsed beams with adjustable spatial dispersion. Ultimately group velocity is tuned at the focal point in order to match the prescribed phase velocity. We also present a dispersive beam expander consisting of a hybrid diffractive-refractive triplet capable of preparing the spatiotemporal response of ultrashort Gaussian pulses to maintain a stationary CEP along the optical axis when focused within dispersive media. Robustness of the optical arrangement is demonstrated upon coupling with immersion microscope objectives.

Acknowledgments

This research was funded by Ministerio de Ciencia e Innovación (grant HU2007-0020) and Generalitat Valenciana (grants GV/2007/043 and GVPRE/2008/005). Carlos J. Zapata-Rodríguez also acknowledges financial support from Ministerio de Ciencia e Innovación (Subprograma de estancias de movilidad de profesores investigadores en centros extranjeros).